ENGINEERING RESEARCH INSTITUTE
UNIVERSITY OF MICHIGAN
ANN ARBOR

REPORT NO. 1

PRELIMINARY REPORT ON THE "CUTTING CHARACTERISTICS OF TITANIUM"

(A Technical Paper Presented Before the ASME, December 3, 1952)

By

L. V. COLWELL

W. C. TRUCKENMILLER

Project M993

U. S. ARMY, ORDNANCE CORPS
CONTRACT NO. DA-20-018-ORD-11918

December, 1952

SUMMARY SHEET

I. Engineering Research Institute, University of Michigan, Ann Arbor, Michigan.

II. U. S. Army, Ordnance Corps.

III. Project No. TB4-15.
Contract DA-20-018 ORD-11918, RAD No. ORDTB-1-12045.

IV. Report No. WAL 401/109-1

V. Priority No. - None

VI. Investigation of machinability of titanium-base alloys.

VII. Object:

The object is to investigate the machinability of commercially pure titanium and three alloys of titanium.

VIII. Summary:

A series of preliminary machining tests were made to evaluate the general characteristics of titanium in relation to SAE 1045 steel and type 304 stainless steel (18-8). The observations include, chip formation, micro-hardness, tool life, and cutting forces.

TECHNICAL REPORT DISTRIBUTION LIST

Copy No.	Contractor
1	Department of the Army Office, Chief of Ordnance The Pentagon Washington 25, D. C. Attn: ORDTB - Res. and Matls.
2-3	Same. Attn: ORDTA - Ammunition Div.
4	Same. Attn: ORDTR - Artillery Div.
5	Same. Attn: ORDTS - Small Arms Div.
6	Same. Attn: ORDTT - Tank Automotive
7	Same. Attn: ORDTU - Rocket Div.
8	Same. Attn: ORDTX-AR - Executive Library
9-10	Same. Attn: ORDIX
11-12	Commanding General Aberdeen Proving Ground Aberdeen, Maryland Attn: ORDTE R. D. and E. Library
13	Commanding General Detroit Arsenal Center Line, Michigan
14-15	Commanding Officer Frankford Arsenal Bridesburg Station Philadelphia 37, Pa.
16	Commanding Officer Picatinny Arsenal Dover, New Jersey
17-18	Commanding Officer Redstone Arsenal Huntsville, Alabama
19	Commanding Officer Rock Island Arsenal Rock Island, Illinois

Copy No.	Contractor
20	Commanding Officer Springfield Armory Springfield, Mass.
21	Commanding Officer Watervliet Arsenal Watervliet, New York
22-23	Central Air Documents Office U. B. Building Dayton 2, Ohio Attn: CADO-D
24-25	Commanding Officer Box CM, Duke Station Durham, North Carolina
26	Chief Bureau of Aeronautics Navy Department Washington 25, D. C.
27	Chief Bureau of Ordnance Navy Department Washington 25, D. C.
28	Chief Bureau of Ships Navy Department Washington 25, D. C.
29	Chief Naval Experimental Station Navy Department Annapolis, Maryland
30	Commanding Officer Naval Proving Ground Dahlgren, Virginia Attn: A. and P. Lab.
31	Director Naval Research Laboratory Anacostia Station Washington, D. C.

Copy No.	Contractor
32	Chief Office of Naval Research Navy Department Washington, D. C.
33	Commanding General Air Materiel Command Wright-Patterson Air Force Base Dayton 2, Ohio Attn: Production Resources MCPB and Flight Research Lab.
34	Commanding General Air Materiel Command Wright-Patterson Air Force Base Dayton 2, Ohio Attn: Materials Lab., MCREXM
35	Director U. S. Department of Interior Bureau of Mines Washington, D. C.
36	Chief Bureau of Mines Eastern Research Station College Park, Maryland
37	National Advisory Committee for Aeronautics 1500 New Hampshire Avenue Washington, D. C.
38	Office of the Chief of Engineers Department of the Army Washington 25, D. C. Attn: Eng. Res. and Dev. Div. Military Oper.
39	U. S. Atomic Energy Commission Technical Information Service P. O. Box 62 Oak Ridge, Tennessee Attn: Chief, Library Branch

Copy No.	Contractor
40	District Chief Detroit Ordnance District 574 E. Woodbridge Detroit 31, Michigan
41	Masaachusetts Institute of Technology Cambridge, Massachusetts Via: Boston Ordnance District
42	Commanding Officer Watertown Arsenal Watertown 72, Massachusetts Attn: Technical Representative
43-44-45- 46-47-48- 49-50	Commanding Officer Watertown Arsenal Watertown 72, Massachusetts Attn: Laboratory
51	Dr. James E. Bryson Office of Naval Research 844 N. Rush Street Chicago 11, Illinois
52	Ford Motor Company 3000 Schaefer Road Dearborn, Michigan Attn: Mr. R. Lesman Supervisor, Development Section Manufacturing Engineering Department Engine and Foundry Division
53-54	Engineering Research Institute Project File University of Michigan Ann Arbor, Michigan

Initial distribution has been made of this report in accordance with the distribution list. Additional distribution without recourse to the Ordnance Office may be made to United States military organizations, and to such of their contractors as they certify to be cleared to receive this report and to need it in the furtherance of a military contract.

PREFACE

This report is the first of some twenty or more reports which will be submitted on the whole machinability program for titanium; these will be followed by a summary report for all phases of the program. Those following in sequence will detail testing procedures and present all original data; interpretation will be conservative until all data have finally been obtained. This report is the only exception to this practice; it is a preliminary review of some of the evidence obtained in the earlier stages of the program. It was presented as a paper before the American Society of Mechanical Engineers at the Hotel McAlpin in New York City on December 3, 1952. Several of the topics presented in the paper are discussed in greater detail in later reports.

CUTTING CHARACTERISTICS OF TITANIUM

(Reprint of a Paper by L. V. Colwell and W. C. Truckenmiller,
Presented to ASME, December 3, 1952

Alloys of titanium combine high strength with relatively light weight and good corrosion resistance. These facts, coupled with rapid increases in supply, have caused considerable speculation not only on the functional applications but also on the fabrication of these alloys for the many products being considered. Machining usually plays an important part in early industrial experience with new metals, since the larger quantities of parts which provide the greatest stimulus for the development of successful forging, casting, and other nonmachining techniques come later. This has been true also with the titanium alloys.

Lacking in precedents for cutting practice, it is understandable that various shops differed widely in their initial attempts to machine these alloys. It is also understandable that many conflicting reports resulted from their efforts. It was said that titanium cut like stainless steel; that it work-hardened rapidly; that it couldn't be tapped; that it couldn't be hacksawed; that it could be hacksawed but it couldn't be cut with abrasive cut-off wheels; etc.

An investigation has been undertaken to evaluate the unique and pertinent cutting characteristics of titanium and its alloys with the final objective of designating necessary changes in commercial practice in regard to tools, size of cut, speed, etc. This paper presents observations from some of the earlier phases of the investigation. These phases were designed to reveal and emphasize those aspects of the problem which would require comprehensive investigation. For the purpose of giving emphasis, as well as serving as a basis for comparison, the paper also presents the results obtained with 18-8 stainless steel and hot-rolled SAE 1045 steel cut under the same conditions as the titanium alloys.

Preliminary Observations

The laboratory phases of the program were preceded by general attempts to cut RC-130B titanium (4% aluminum and 4% manganese) by ordinary shop methods. By this approach it was possible to turn, mill, shape, drill, ream, hacksaw, bandsaw, form-turn, and part this alloy. It was observed that feeding forces were unusually high, temperatures were high, chips were abnormally thin, and exceptional machine rigidity was required both to start and to sustain cutting.

Figure 1 shows the results obtained from the first laboratory study of the program. These are photomicrographs of chip formation specimens prepared in a shaper by mounting 3-inch long specimens in a vise so that the tool lacked about 1/2 inch of completing the full length of cut, thus leaving the chip intact with the work specimen. All three pictures are at the same magnification; consequently, the first and most obvious impression is the very thin chip produced by the RC-130B titanium compared to both the type 304 stainless steel and the cold-rolled SAE 1020 steel. This difference is accompanied by corresponding differences in the shear angle, as would be expected. The titanium shows a large shear angle relative to the direction of cutting, while both the stainless and the SAE 1020 steels cut with much smaller angles.

The third factor of interest in a comparative test of this type is the work-hardening or distortion of the microstructure. No distortion is visible on the titanium except in the chip and even that is pretty well localized in the distinct cleavage lines. Microscopic examination showed no distortion of the microstructure near the cut surface except at 1000 magnification. The distortion in the steels, however, is so great that it is difficult to recognize many features of the original structure in the chip. Initial slippage is evident in the stainless steel in some grains quite remote from the shear zones, indicating the extent and depth of penetration of the stress. The change in hardness associated with this distortion is substantial, as is pointed out later in Figures 2 to 4 inclusive.

Certain tentative conclusions can be inferred from the comparative information shown in Figure 1. They are that when cutting grade 130B titanium

a. unit pressure on the cutting tool will be higher,
b. temperature at the tip of the cutting tool will be higher, and
c. surface roughness resulting from "smear" on the work surface will be less.

The first of these conclusions is evident from the very small contact area between the chip and the cutting tool compared to those obtained with both the 18-8 stainless and the low-carbon steel at the same size of cut and cutting conditions.

The second conclusion that the temperature will be greater is influenced by two factors. First, the presence of a built-up edge with the steels reduces the temperature level before the heat reaches the the cutting tool. Secondly, also due to the built-up edge, the heat is distributed over a considerably greater area, thus reducing the concentration of heat and the probability of destructively high temperature. The third conclusion is obvious, since no "smear" metal appears on the cut surface.

Figures 2, 3, and 4 show the results of microhardness surveys of the same machining specimens as those shown in Figure 1. The unstrained material of the SAE 1020 steel showed a hardness of a little over 100, while the built-up edge was hardened to an average of 426, an increase of over 300%. Two separate regions of the chip showed average hardness numbers of 338 and 360 respectively with increasing amount of distortion. It is to be noted also that work-hardening was manifest in higher hardness readings to a depth of at least 0.016 inch.

Figure 3 shows similar hardness readings for the type 304 stainless steel. The body hardness averaged 260, while the built-up edge averaged 494; an increase of 90%. The chip showed an average of 400, or an increase of 54% over the body hardness.

The hardness traverse results from titanium 130B are shown in Figure 4. The body hardness averaged 376, while the chip averaged 551, an increase of only 46% compared to 54% and 250% for the 18-8 and SAE 1020 respectively.

Effect of Tool Rake Angle and Surface Finish

The absence of a built-up edge makes the large shear angle a serious problem in view of the high temperatures and pressures that can result from this combination. Since the presence of a built-up edge can reduce both temperature and pressure on the cutting tool, an attempt was made to induce one for this purpose even though some sacrifice in surface finish might have to be made. Figure 5 shows the results of this attempt.

Using the same general procedure as in Figure 1, two sets of shaper tools were prepared representing a range of rake angles and two levels of surface roughness. Each set of tools consisted of three tools. The first set was ground by the most careful methods available, resulting in a roughness level of 0-1.3 microinches. The second set, designated as "rough-ground"

tools, were machine ground with coarse grit wheels, resulting in a roughness level of 31-50 microinches; this level is about as rough as would ordinarily be accepted in a shop. In both instances the grinding marks were oriented parallel to the cutting edge so as to exert the maximum influence on pressure welding.

It will be noted that all chips produced by these tools were type 1 segmental chips like those produced earlier by the 130B titanium. The must obvious result is that the attempt to produce a built-up edge failed, at least in the sense that a built-up-edge is retained. However, it will be noted that something comparable to a built-up edge was trapped at least momentarily with the -15°-rake rough-ground tool, as shown at the lower left in the figure. It is not believed that this phenomenon persisted for any significant period of time, although there is evidence that it may have occurred relatively frequently, but perhaps only in a partial state of development. It will be noted that shear cleavage surfaces occur at least once in every chip in Figure 5 except those obtained with the +20°-rake tools. These surfaces are oriented obliquely relative to the underside of the chip. Further reference is made to this phenomenon later in connection with Figures 7 and 9.

The shear angles were measured for each of the conditions represented in Figure 5; the results are shown in Table I below.

TABLE I

SHEAR ANGLES FOR RC 130B TITANIUM CUT DRY

	Rake Angle		
	-15°	0°	+20°
Smooth-Ground Tools	22	31	42
Rough-Ground Tools	22	29	43

If the current theories relating shear angle, coefficient of friction, and rake angle are correct, then the wide difference in rougheness between the two sets of tools did not produce any appreciable change in the effective coefficient of friction. However, there is an obvious difference in the frequency and pitch of the cleavage surfaces, indicating that the difference in roughness did exert some influence and it is difficult to comprehend how this could be effected except through a change in either the level or the behavior pattern of friction.

Reference to Table I shows that the increments of shear angle are approximatley one-half the corresponding increments of rake angle. The calculated coefficient of friction from cutting force tests made on RC-130B titanium is approximately 1.0. If it is assumed that the rake angle has little effect on the coefficient of friction, then the data in Table I conform quite closely to the original theory of Ernst and Merchant[1] and the modified theory of Merchant[2] wherein the relationship of the shear angle (ϕ), the friction angle (β), and the rake angle (α) are respectively expressed as

$$\phi = 45 - \beta/2 + \alpha/2 \qquad (1)$$

and

$$\phi = \frac{\cot^{-1}(K)}{2} - \beta/2 + \alpha/2, \qquad (2)$$

where K expresses the rate of influence of normal stress σ on the shear stress τ as given in the equation $\tau = \tau_o + K\sigma$. The maximum value of the first term of Equation (2) is 45° when $K = 0$.

Substituting $\beta = 45°$ and $\alpha = 0°$ into Equation (1) gives:

$$\phi = 45° - 45°/2 = 22\text{-}1/2°.$$

This is substantially lower than either the 29° or the 31° shown for the zero-rake-angle tools. Similar substitutions into the shear angle equations proposed by others lead to the results of Table II.

TABLE II

CALCULATED SHEAR ANGLE

Author	Bibl. Ref.	Equation	ϕ, °
Stabler	3	$\phi = 45 - \beta + \alpha/2$	0
Lee and Shaffer	4	$\phi = 45 - \beta + \alpha$	0
Huchs	5	$\phi = 45 \frac{-\tan^{-1} 2\mu}{2} + \alpha$	12

It can be seen from Table II that some of the other current theories are in substantially less agreement than that of Ernst and Merchant. Recently, Shaw, Cook, and Finnie[6] produced an extension of the theory wherein a new term η' was added as follows:

$$\phi = 45 + \eta' - \beta + \alpha.$$

It is claimed that this term (η') reflects the influence of the degree of constraint, manifest in the rake angle, on the effective hardness of the chip and that this in turn affects the coefficient of friction in the usual manner to result in higher coefficients with higher rake angles. η' cannot be determined directly from the photomicrographs in Figure 5, but it is related to the oblique angle which the plane of principal shear makes with the bottom of the chip. This is designated as the angle η and is related to η' as follows:

$$\phi = \eta + \alpha + \eta' \tag{3}$$

$$\eta = 45 - \beta \tag{4}$$

$$\phi = 45 + \quad ' - \beta + \alpha . \tag{5}$$

Therefore, the angle η' should be equal to zero if the coefficient of friction is equal to 1.0. The average value of η is 20°, for which the friction angle would have to be equal to 25° or μ = 0.466 to conform to the theory. If it were assumed that μ = 0.466, then η' would be approximately -13° and ϕ would be equal to 7°.

Thus it appears that there is something unique about the cutting behavior of titanium, since the theories advanced to date predict the cutting behavior for other metals much more accurately than they do for titanium. It is quite possible that these new alloys may, by contrast, provide the information needed to reveal the significant discrepancies in existing theory. However, it is not the purpose of this paper to dwell on this point, although some additional evidence along this same line will be presented in Figure 9 in the hope that it may be useful in providing leads for further extension of metal-cutting theory.

Microscopic examination of the specimens shown in Figure 5 revealed significant differences in the regularity and smoothness of the cut surface as they appear in cross section. This led to examination of the surface at the point where the tool entered the cut. The results are shown in Figure 6 for the smooth-ground tools. They indicate that there is an initial loss of depth of cut proportional to the force normal to the cutting direction. In the case of the +20° rake angle, the force is low enough relative to inherent damping so that the pulsating nature of the cutting force is reflected in the work surface beyond the entrance. On the other hand, this phenomenon appears to be damped out completely with both the 0° and the -15° rake angles. The loss of depth of cut is substantially greater than that observed in steel despite the fact that the force in the direction of cutting is substantially less than for a steel of corresponding strength.

This may be due to an exceptionally high coefficient of friction which has not been established as yet, or it may be related to residual cutting forces at zero size of cut, considered as a limit approached from finite sizes of cut. An interesting approach to this aspect of the problem was proposed recently by Thomsen, Lapsley, and Grassi.[7]

Figure 7 shows two pictures of additional portions of the chips obtained with the smooth-ground tools. These pictures reveal the persistence of the surfaces of principal shear as they appear adjacent to the underside of the chip. This is the only instance in the authors' experience where this phenomenon has been observed except in the case of low-carbon steel cut at very low speeds; even in the latter instance the indication has been very superficial.

In the lower part of Figure 7 there is a sketch of the stress field indicated by Shaw, Cook, and Finnie.[6] The mutual perpendicular dashed lines represent the surfaces of principal shear peculiar to the theory advanced by these authors. The similarity of the cleavage surfaces, shown in the photomicrographs, to the orientation of one of the surfaces of principal stress in most interesting.

Chip Formation vs Titanium Alloy

Chip formation studies with shaper cuts were the first to be made when the Ti-75A and Ti-150A grades of titanium because available. However, the test conditions were revised to overcome objections to some of the earlier tests on RC-130B. Principally this revision consisted of an increase of the depth or thickness of cut from 0.005 inch to 0.015 inch to minimize the effect of the blunting which was evident near the cutting edge. The results of these tests are shown in Figure 8. It will be noted that, as before, the RC-130B produces a distinct Type 1 segmental chip, while the Ti-150A produces a distinct Type 2 chip. The Ti-75A is intermediate between these two in that it produces substantially a smooth continuous chip but it also shows some tendency toward segmentation. All three alloys are similar in regard to relatively thin chips and correspondingly large shear angles. In this respect, RC-130B still produces the largest shear angle, while the Ti-75A gives the least and the Ti-150A is intermediate. The basis for the rather extreme difference in behavior as between the RC-130B and the Ti-150A is not evident from any data obtained up to this time. This information is presented for whatever intrinsic value it may have and in the hope that others may contribute toward an explanation of the differences in behavior.

The Mechanism of Chip Formation

A further extension of the chip formation tests is shown in Figure 9. Two specimens of each material were prepared for shaper cuts. They were 0.150 inch thick, 1/2 inch high, and 5/8 inch long. In addition, a 30° by 0.075-inch wide bevel was machined on one corner parallel to the 5/8-inch length. The 1/2-inch by 5/8-inch side opposite the bevel was scribed with a 0.003-inch square grid using gage blocks and a gage scriber. In conducting the tests, each pair of specimens was clamped in a vise with the scribed surfaces contacting each other under the pressure exerted by the vise. After a clean-up cut, a test cut was made in such a manner that the tool was stopped midway along the 5/8-inch length. A two-part chip was formed at a depth of 0.015 inch and a total width of approximately 0.200 inch. The cutting tool was a 1-1/4 inch square, solid tool ground for 0° rake angle. Strain gages were mounted directly on the tool so that both the thrust and cutting components could be indicated. The results are shown in Table III.

TABLE III

CUTTING FORCES FOR GRID SPECIMENS

Work Material	Forces-Pounds F_c	Forces-Pounds F_n	Coefficient of Friction	Thickness of Cut	Width of Cut
Ti-75A	851	840	.99	.0127	.186
RC-130B	667	652	.98	.0164	.186
Ti-150A	894	830	.93	.0132	.163
304 S.S.	1268	1010	.80	.0086	.192
SAE 1045	1038	760	.73	.0146	.186

It will be noted that the coefficient of friction for the titanium alloys is approximately 1.0, while it is significantly lower for the two other alloys.

Pictures of the grid surfaces of the specimens are shown in Figure 9. The use of polarized light in making the pictures apparently assisted in identifying the existence of substantial plastic strain ahead of the usual shear plane. It is distinctly evident in all three types of titanium; it

was even more evident and more extensive in type 304 stainless and SAE 1045 steel, although pictures of these specimens were not included in this figure. No attempt will be made at this writing to extend the theory to explain the influence of this phenomenon on the cutting behavior. However, it is appropriate to call attention to certain implications regarding current theories.

Present theory assumes that the metal remains elastic until it enters the shear zone identified with what has commonly been called the shear plane; this is clearly not the case at all if the evidence shown in Figure 9 is representative of metal cutting. Assuming the evidence to be valid, it means that the stress level has gone beyond the yield or flow point, thus indicating that it is substantial and must be taken into consideration in any theory relating the determinants of the shear angle and cutting forces.

Further, the fact that a differential volume of metal passes through such a stress field prior to the shear plane means that it can undergo considerable strain hardening. In addition to this, the shape of the stress field indicates the possibility of different amounts of strain-hardening resulting from different paths through the field. Assuming the existence of these possibilities, it means finally that there may be a considerable variation in the shear flow stress across the shear plane, resulting in higher average stress and a major shift in the position of the resulting forces. Future extensions of the theory will be more difficult, since the problem cannot be treated either as a plane stress problem or as a plane strain problem. However, despite these difficulties, the very nature of the new evidence shows promise of assisting greatly in explaining apparent deviations of existing data when considered in the light of current theory. It is to be hoped that the uniqueness of the cutting behavior of titanium will shed further light on the correct theory.

Cutting vs Physical Properties

The tensile properties of the several materials being investigated in the machining program are shown in Table IV. In the conduct of such a program, trial correlations are made as a routine matter. That particular approach produced the results shown in Figure 10. This figure correlates the shear angle ϕ with a ratio formed by the product of the ratio of per cent reduction of area to per cent elongation and yield point to tensile strength. The values of shear angle as plotted are averages obtained from multiple shaper tests in which different lubricating conditions were used. Thus the averages also represent average performance. There is no obvious basis for this correlation and so it is presented in the interest of stimulating discussion and bringing forth additional evidence either to confirm or disprove it as a valid trend.

TABLE IV

TENSILE PROPERTIES OF WORK MATERIALS

Material	Sample Number	Yield Strength*	Tensile Strength	Breaking Strength	Per Cent Elongation	Per Cent Reduction of Area
304 S. S.	1	37,500	85,500	55,000	64.5	77.4
304 S. S.	2	41,000	85,700	54,500	62.7	77.4
SAE 1045	1	48,600	101,200	91,000	21.5	33.0
SAE 1045	2	48,800	101,800	92,500	21.7	34.4
SAE 1045	3	53,000	101,700	93,500	22.5	34.6
Ti-75A	1	60,000	82,000	66,000	28.0	47.1
Ti-75A	2	57,400	82,100	65,500	28.5	48.6
Ti-75A	3	57,700	82,000	65,500	27.7	45.8
RC-130B	1	139,000 **	155,500	122,500	18.5	41.9
RC-130B	2	139,400 **	155,000	126,200	17.7	37.9
RC-130B	3	139,400 **	155,200	121,700	18.3	45.3
Ti-150A	1	131,700	141,000	97,200	25.0	55.8
Ti-150A	2	132,500	140,200	99,200	24.7	54.5
Ti-150A	3	130,000	140,400	97,400	25.0	55.1

* Yield strength determined by 0.2% offset method

** Yield point value

Table V presents the Brinell hardness numbers and the Meyer strain-hardening exponents for the materials included in Table IV. The Meyer exponents were obtained with loads varying from 1000 to 3000 kg in 500-kg increments.

TABLE V

BHN AND MEYER EXPONENTS

Work Material	BHN*	Meyer Exponent, n**
Ti 75A	217	2.41
RC 130B	331	2.37
Ti 150A	302	2.27
304 S.S.	174	2.32
SAE 1045	201	2.25

* 3000-kg Load

** Load = ad^n

Tool-Life Properties

Eventually, most metal-cutting studies lead to tool-life tests, since it is this property which has the greatest commercial significance. A great many tool-life tests in turning have been run to evaluate the effect of side rake angle. The results obtained to date are summarized in Figure 11. The curves of tool life vs rake angle show the existence of a fairly sharp optimum for each of the four metals. It should be noted that only one size of cut was used and the tool shape was held constant except for the side rake angles. This is not a complete picture, but it does appear to indicate that optimum rake angles when cutting with high-speed-steel tools are larger than was expected. It is interesting to speculate whether there is any dependent relationship of this fact to the larger shear angles also peculiar to titanium. The cutting speeds represented in Figure 11 are those which result in a tool life of one hour with the optimum rake angle. These speeds are summarized in Table VI.

TABLE VI

CUTTING SPEEDS FOR ONE-HOUR TOOL LIFE
AT OPTIMUM RAKE ANGLE

Work Material	V_{60}, fpm
RC-130B	48
Ti-150A	74
304 S.S.	99
SAE 1045	187

Summary

A. Titanium demonstrates cutting properties that are unique in the degree or magnitude of the porperty. Some of these are:

1. It work-hardens more superficially than some other metals.
2. It has little or no tendency to form a built-up edge.
3. It forms very thin chips relative to the thickness of the cut and thus tends to intensify problems related to pressure and temperature.
4. Specific energy consumption is of the same magnitude as for medium-carbon and low-alloy steels.

B. A substantial field of plastic strain has been revealed ahead of the fimiliar shear zone. This presents many possibilities for further investigation and extension of metal-cutting theory.

C. There appears to be a good correlation between shear angle and tensile properties of metals including titanium. However, the correlation may be indirect, since there is no obvious basis for such a dependency.

D. The probable higher temperatures and pressures are at least partially confirmed by relatively low cutting speeds for a constant tool life compared to SAE 1045 steel.

Grateful acknowledgement is made to the Watertown Arsenal for permission to disclose this information and to the Laboratory staff for cooperation and encouragement in carrying out this investigation.

BIBLIOGRAPHY

1. "Chip Formation, Friction and High-Quality Machined Surfaces", by H. Ernst and M. E. Merchant, Surface Treatment of Metals, American Society for Metals, p. 299, 1941.

2. "Mechanics of the Metal Cutting Process" by M. E. Merchant, Journal Applied Phys. 16, 267, 318 (1945).

3. "The Fundamental Geometry of Cutting Tools", by G. V. Stabler, Proceedings of the Institute of Mechanical Engineers (London) 165, 14, 1951.

4. "The Theory of Plasticity Applied to a Problem of Machining", by E. H. Lee and B. W. Shaffer, ASME Preprint 51-A-5, 1951.

5. "Plastizitätsmechanische Grundlagen und Kenngressen der Zerspannung", by H. Huchs, Dr. Ing disseitation, Technische Holhschule, Aachen, February 1951.

6. "The Shear Angle Relationship in Metal Cutting", by M. C. Shaw, N. H. Cook, and I. Finnie, ASME Preprint No. 52-SA-51, 1952

7. "Deformation Work Absorbed by the Work Piece During Metal Cutting," by E. G. Thomsen and J. T. Lapsley, Jr., and R. C. Grassi, ASME Preprint 52-F-24, 1952.

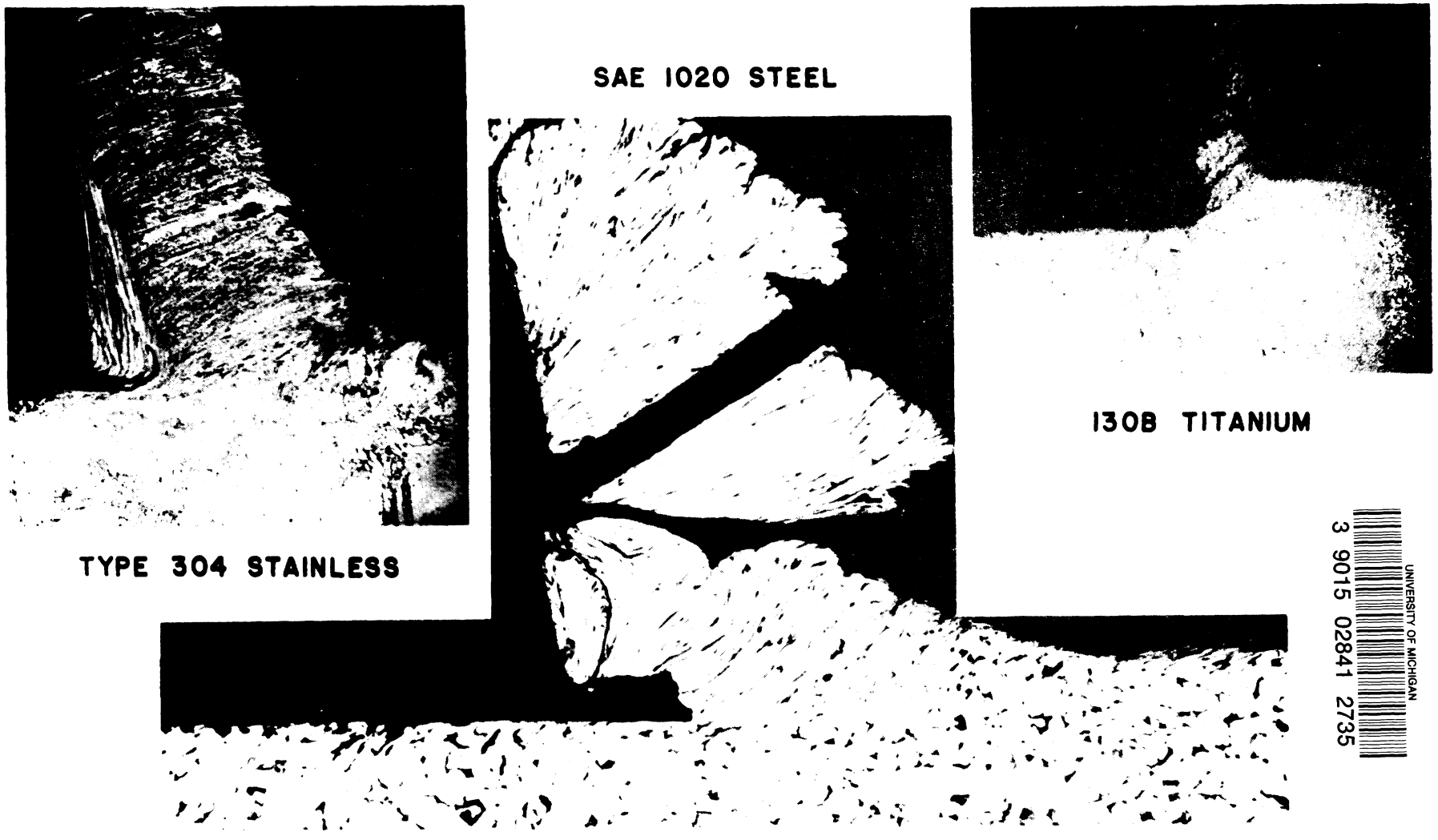

FIGURE I. CHIP FORMATION VERSUS MATERIAL CUT. CUTTING CONDITIONS: AT END OF SHAPER STROKE WITH 9" STROKE, 9 STROKES PER MINUTE, 0.005" DEPTH OF CUT, 0.250" WIDTH OF CUT. TOOL SIGNATURE: 8,0,6,3,0,0,0. MAGNIFICATION 50 X. S.A.E. 1020 STEEL, NITAL ETCH; TYPE 304 STAINLESS STEEL, ELECTROLYTIC CHROMIC ACID ETCH; TYPE 130 B TITANIUM, 48% HYDROFLUORIC ACID IN GLYCERINE ETCH.

426
417
427
427
433
} 0.001" INTER-VALS

340
368
356
362
361
361
373
362

325
323
343
351
335
342
356
331
256
237
209
} 0.001" INTERVALS

} 0.005"

176

} 0.010"

131

} 0.010"

113

NOT SHOWN IN PHOTOGRAPH

MACHINED SURFACE DIRECTION OF CUTTING

363
361
326
307
301
269
213
} 0.001" INTERVALS

} 0.002" INTERVALS

186

182

} 0.005"

147

216
211
203
200
241
} 0.001" INTERVALS

136

} 0.002" INTERVALS

159

} 0.005"

126

FIGURE 2. TUKON HARDNESS OF CUTTING REGION FOR S.A.E. 1020 STEEL. CUTTING CONDITIONS: SAME AS FIGURE 1. TUKON OPERATION: 100 GRAM LOAD, KNOOP PENETRATOR. TESTS MADE ON SAME SECTION OF S.A.E. 1020 STEEL SHOWN IN FIGURE 1.

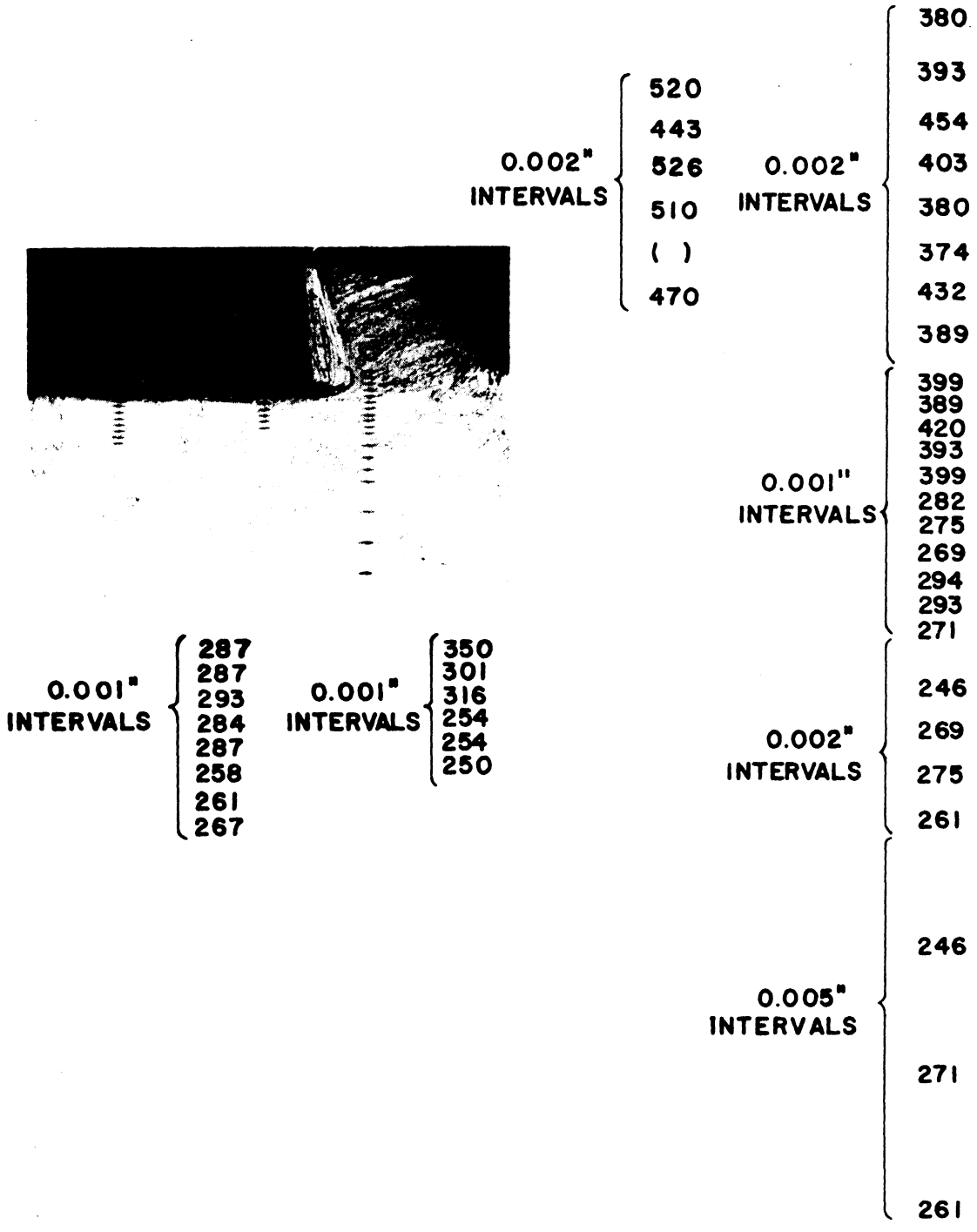

FIGURE 3. TUKON HARDNESS OF CUTTING REGION FOR TYPE 304 STAINLESS STEEL. CUTTING CONDITIONS: SAME AS FIGURE 1. TUKON OPERATION: 100 GRAM LOAD, KNOOP PENETRATOR. TESTS MADE ON SAME SECTION OF TYPE 304 STAINLESS STEEL SHOWN IN FIGURE 1.

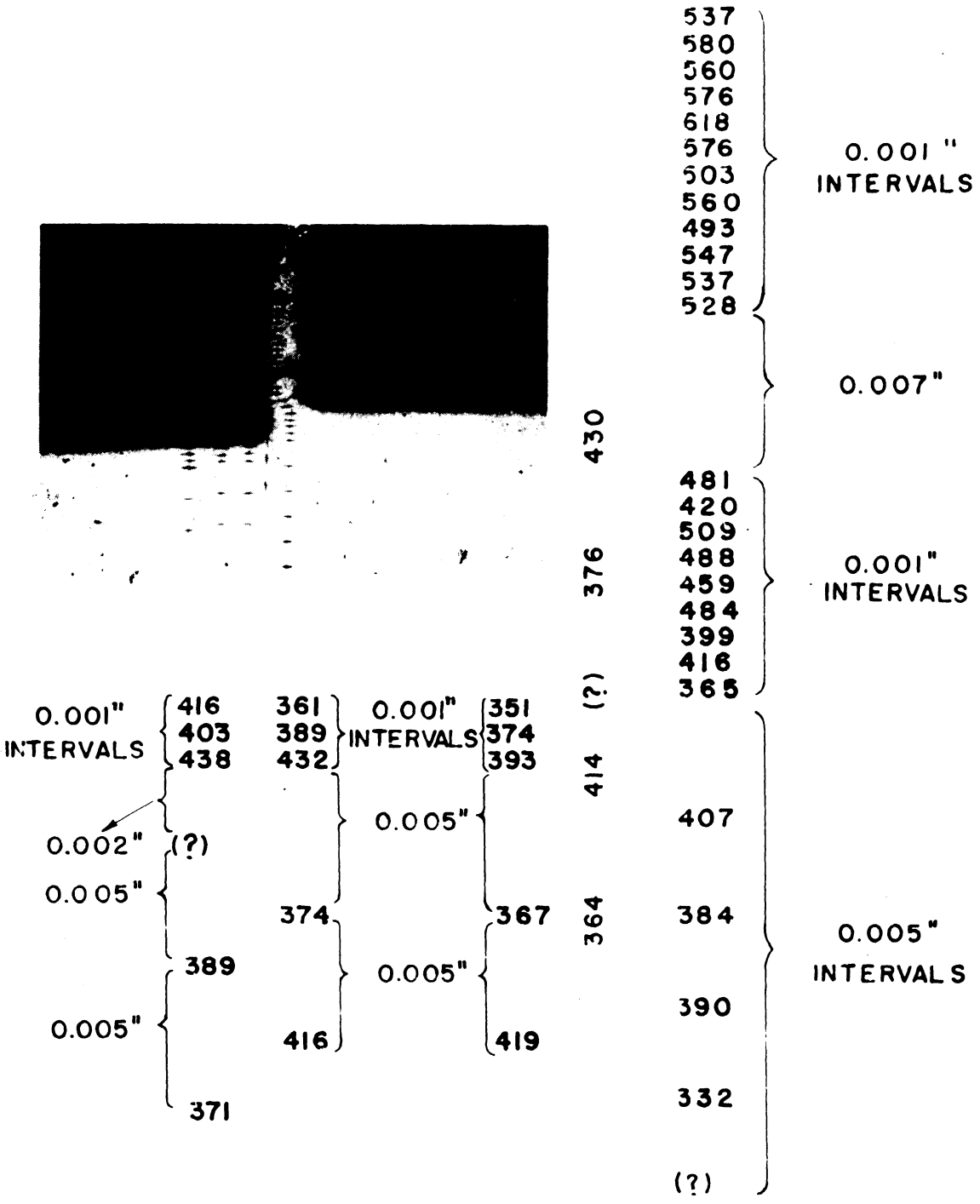

FIGURE 4. TUKON HARDNESS OF CUTTING REGION FOR TYPE 130 B TITANIUM ALLOY. CUTTING CONDITIONS: SAME AS FIGURE 1. TUKON OPERATION: 100 GRAM LOAD, KNOOP PENETRATOR. TESTS MADE ON SAME SECTION OF TYPE 130 B TITANIUM ALLOY SHOWN IN FIGURE 1.

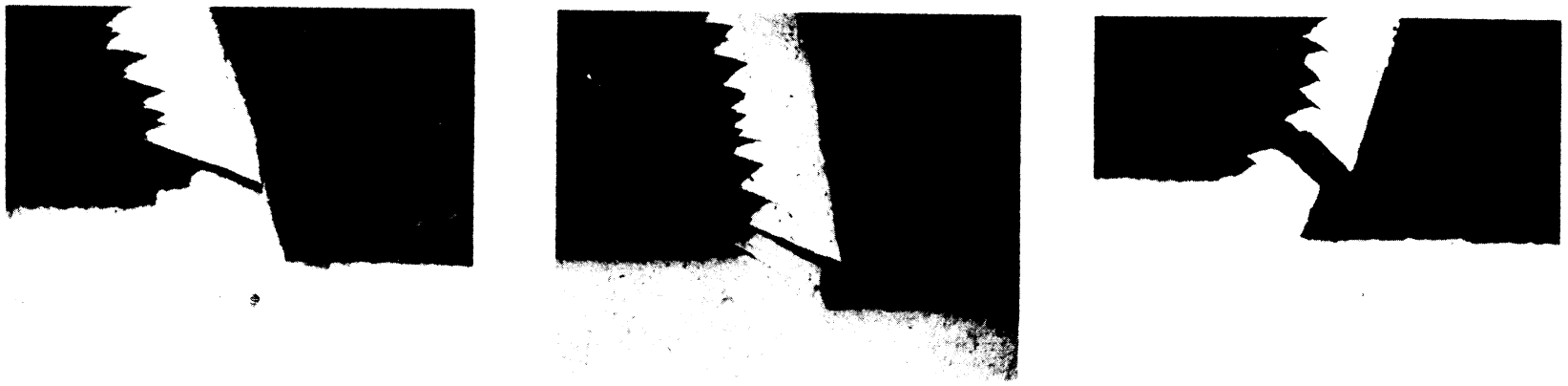

-15° RAKE 0° RAKE +20° RAKE

FINISH GROUND TOOLS.

-15° RAKE 0° RAKE +20° RAKE

ROUGH GROUND TOOLS.

FIGURE 5. CHIP FORMATION VERSUS TOOL RAKE ANGLE AND SURFACE FINISH FOR TYPE 130 B TITANIUM ALLOY. ROUGH GROUND TOOLS 31 - 50 MICRO - INCHES AND FINISH GROUND TOOLS 0 - 1.3 MICRO - INCHES SURFACE ROUGHNESS. CUTTING CONDITIONS : AT END OF SHAPER STROKE, 9" STROKE, 9 STROKES PER MINUTE, 0.005" DEPTH OF CUT, 0.250" WIDTH OF CUT. MAGNIFICATION : 50 X.

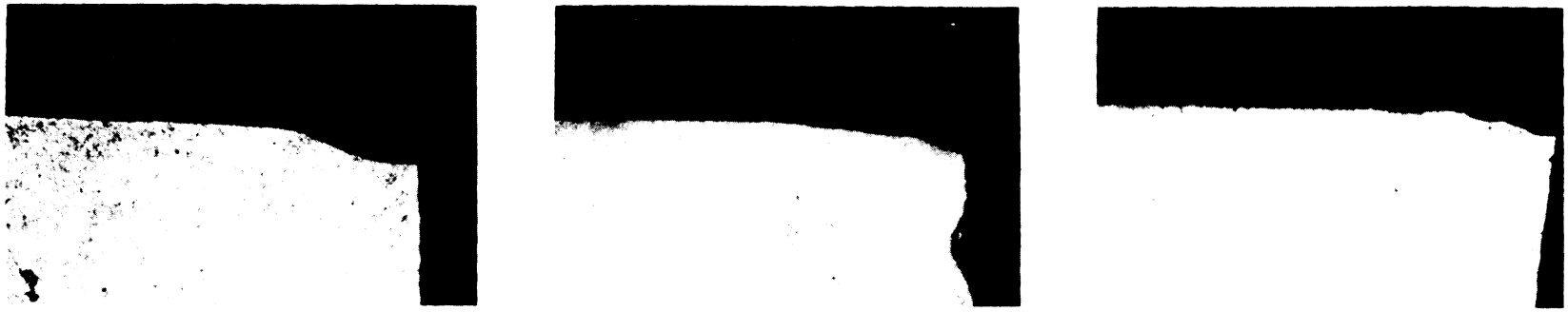

-15° RAKE

0° RAKE

+20° RAKE

FIGURE 6. ENTRANCE CONDITIONS (SHAPER CUT) VERSUS RAKE ANGLE FOR TYPE 130 B TITANIUM ALLOY USING FINISH GROUND TOOLS. CUTTING CONDITIONS AND WORK PIECE ARE THE SAME AS IN FIGURE 5. MAGNIFICATION 50 X .

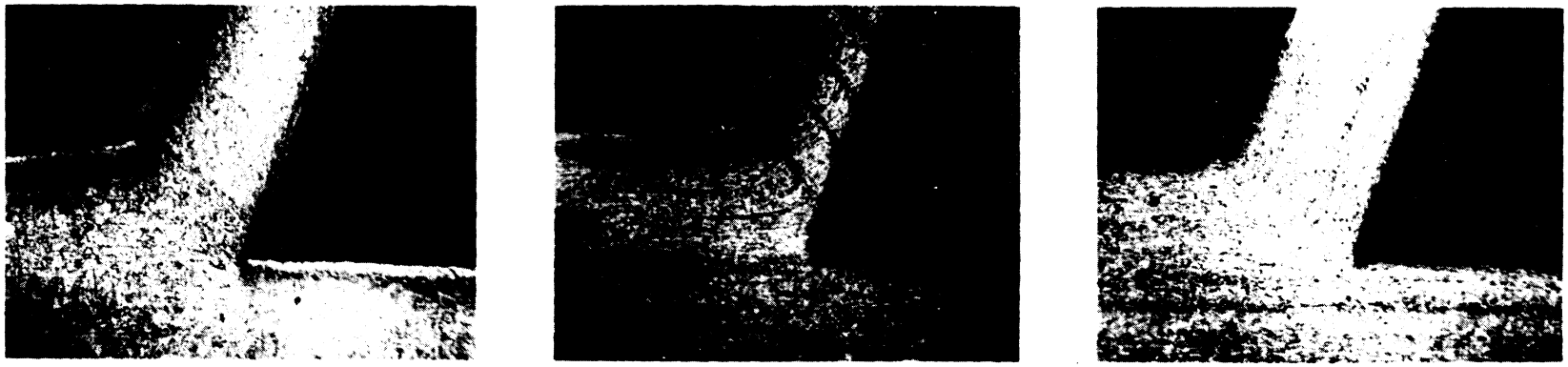

TI. 75A

RC. 130B

TI. 150A

FIGURE 8. CHIP FORMATION VERSUS TITANIUM ALLOY FOR ALLOYS 75 A, 130 B, AND 150 A. CUTTING CONDITIONS: AT END OF SHAPER STROKE, 4" STROKE, 9 STROKES PER MINUTE, 0.015" DEPTH OF CUT, 0.250" WIDTH OF CUT. BACK RAKE ANGLE OF TOOL + 20 °. MAGNIFICATION: 50 X .

426
417
427
427
433
} 0.001" INTER-VALS
340
368
356
362
361
361
373
362

325
323
343
351
335
342
356
331
256
237
209
} 0.001" INTERVALS

} 0.005"

176

} 0.010"

131

} 0.010"

113

NOT SHOWN IN PHOTOGRAPH

MACHINED SURFACE DIRECTION OF CUTTING

363
361
326
307
301
269
} 0.001" INTERVALS

213

} 0.002" INTERVALS

186

182

} 0.005"

147

216
211
203
200
241
} 0.001" INTERVALS

136

} 0.002" INTERVALS

159

} 0.005"

126

FIGURE 2. TUKON HARDNESS OF CUTTING REGION FOR S.A.E. 1020 STEEL. CUTTING CONDITIONS: SAME AS FIGURE 1. TUKON OPERATION: 100 GRAM LOAD, KNOOP PENETRATOR. TESTS MADE ON SAME SECTION OF S.A.E. 1020 STEEL SHOWN IN FIGURE 1.

TI. 75A

TI. 150A

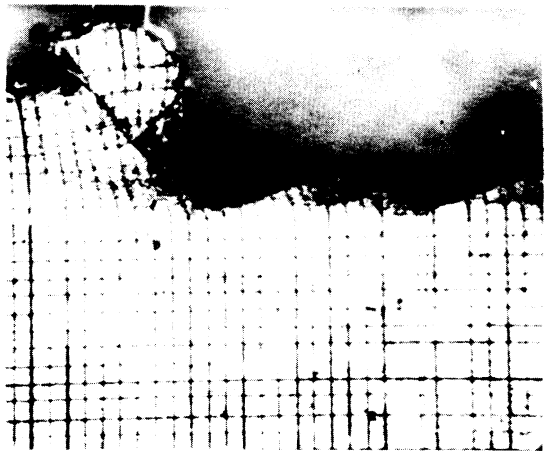

TI. 130B

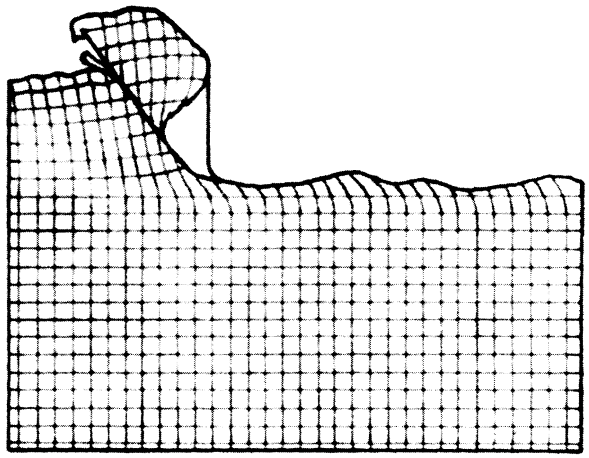

TI. 130B

FIGURE 9. GRID SPECIMENS SHOWING UNIT DISTORTION AND EVIDENCE OF LATERAL STRESS IN CHIP AND WORK MATERIAL FOR THREE TITANIUM ALLOYS. GRID SPACING 0.003" IN BOTH DIRECTIONS. LOWER RIGHT FIGURE IS A TRACING OF LOWER LEFT FIGURE (130 B). CUTTING CONDITIONS: SAME AS FIGURE 8 EXCEPT TOTAL WIDTH WHICH WAS 0.200" RAKE ANGLE OF TOOL = 0°. MAGNIFICATION 50X. PHOTOGRAPHED WITH POLARIZED LIGHT.

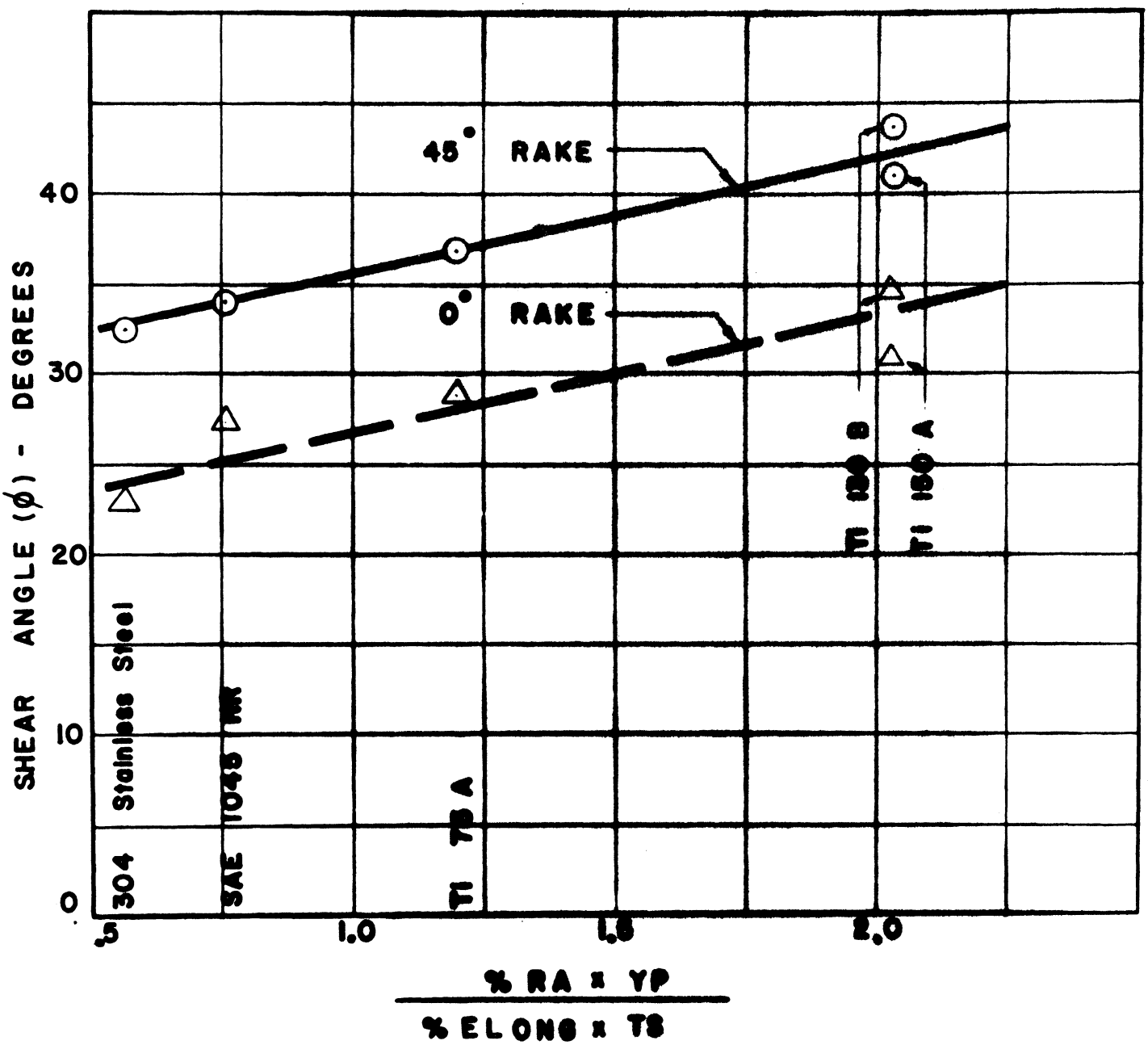

FIGURE 10. AVERAGE SHEAR ANGLE AS A FUNCTION OF TENSILE PROPERTIES FOR FIVE MATERIALS, SEVERAL DEPTHS AND WIDTHS OF CUT, USING CARBON TETRACHLORIDE, WHITE MINERAL OIL, SULPHURIZED OIL, AND DRY CUTTING.

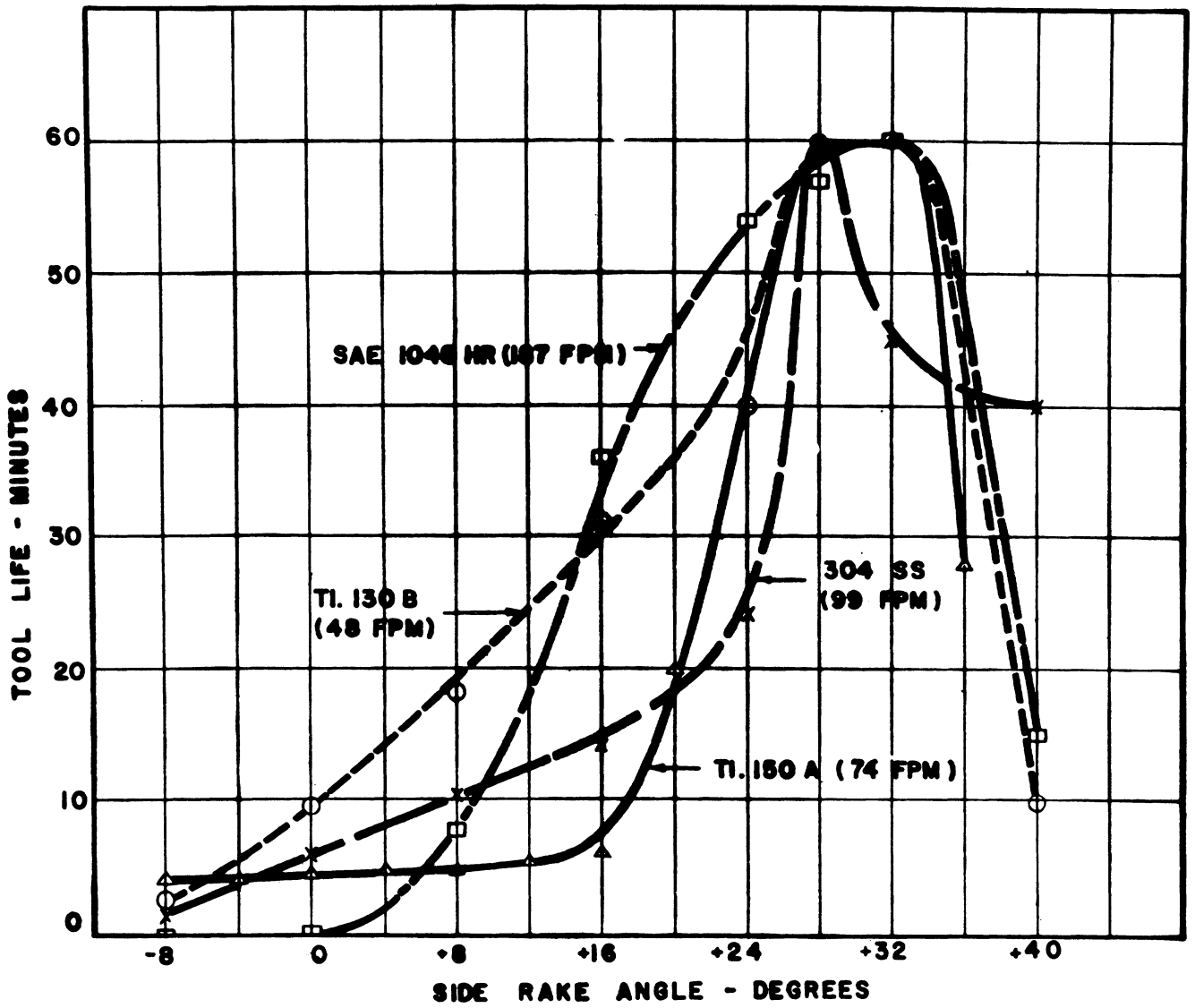

FIGURE 11. EFFECT OF SIDE RAKE ANGLE ON TOOL LIFE IN TURNING FOR FOUR MATERIALS.

TOOL MATERIAL: 18-4-1 H.S.S. FEED: 0.006 IPR.
TOOL SHAPE: 0, VARIABLE, 6, 6, 6, 15, 0.010"
DEPTH OF CUT: 0.050" CUTTING FLUID: DRY